

Easy-to-implement hp -adaptivity for non-elliptic goal-oriented problems

Felipe Vinicio Caro Gutiérrez^{2,1}

Supervisors: David Pardo^{1,2,3}, Elisabete Alberdi¹

¹University of the Basque Country (UPV/EHU), Bilbao, Spain

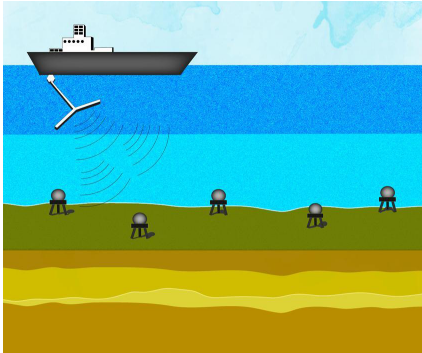
²Basque Center for Applied Mathematics (BCAM), Bilbao, Spain

³Ikerbasque, Bilbao, Spain

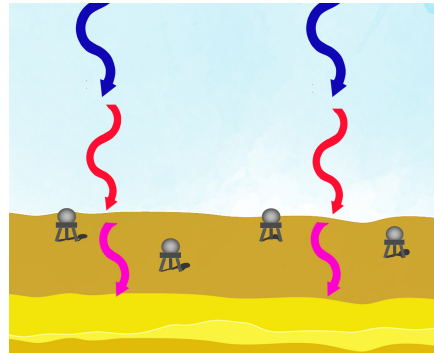
29 November 2023, Leioa



Electromagnetic (EM) Applications



(a) CSEM (artificial source)

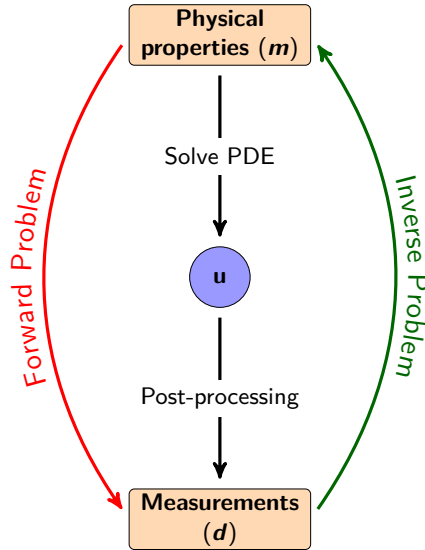


(b) MT (natural source)

Objective

Objective: To obtain the **conductivity/resistivity** distribution of the Earth's subsurface.

Overview of Forward and Inverse Problems



Definitions

\mathcal{F} : Forward Operator
 $\mathbf{m} \mapsto \mathbf{d}$

\mathcal{I} : Inverse Operator
 $\mathbf{d} \mapsto \mathbf{m}$

\mathcal{I}_ϕ : Neural Network approximation of \mathcal{I}

Generation of Massive Databases

Objective

Building the **Inverse Operator** (not just evaluating it).

Loss Function and Training

Find \mathcal{I}_{ϕ^*} such that

$$\phi^* = \arg \min_{\phi \in \Phi} \sum \|(\mathcal{F} \circ \mathcal{I}_\phi)(\mathbf{d}_i) - \mathbf{d}_i\|^2$$

where evaluating \mathcal{F} is **expensive!**

Difficulties

- ① We need a Forward Solver \mathcal{F} for **any parameterization** (model).
- ② A **huge number** of evaluations needed **to train** the DNN.

Solution

- ① Approximate the Forward Operator with a **Neural Network**.

Traditional Numerical Methods in Geophysics

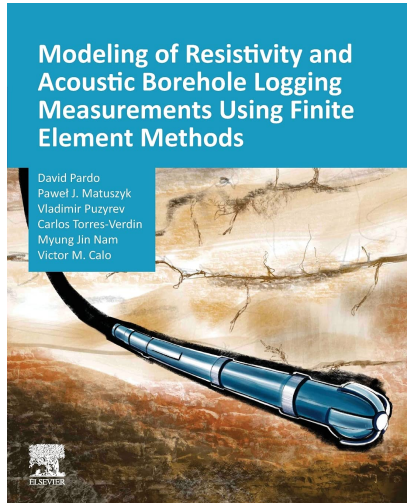


Figure: Published in 2021

Numerical Methods

- Finite Element method
- Finite Difference method
- Finite Volumes method
- Integral methods
- Semi-analytical methods

Outline

- ① Goal-Oriented hp -adaptivity for non-parametric PDEs
 - Why hp -adaptivity?
 - Goal-Oriented coarsening strategy
 - 1D Numerical results for Goal-Oriented h - and p -adaptivity
 - 2D Numerical results for hp -adaptivity
 - 3D Numerical results for hp -adaptivity
- ② Goal-Oriented hp -adaptivity for parametric PDEs.
 - Database generation for DL inversion
- ③ Main Achievements
- ④ Conclusions and Future Work

Goal-Oriented hp -adaptivity for non-parametric PDEs

Why hp -adaptivity?

Advantages

hp -adaptive FEM achieves exponential convergence rates

Precise mesh refinement near singularities

Smaller meshes with higher accuracy per number of degrees of freedom

Limitations

Solution accuracy heavily mesh-dependent, requiring precise mesh design

Increasing accuracy leads to prohibitive computational costs

Main Ingredients

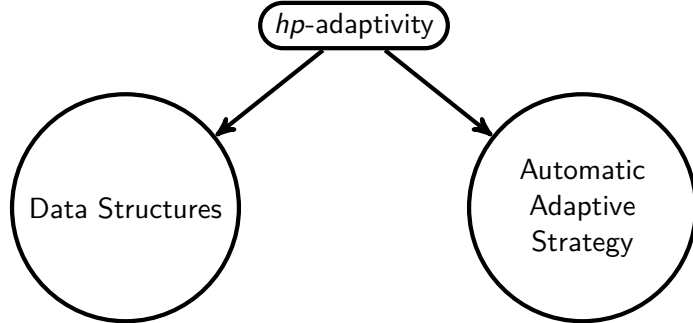
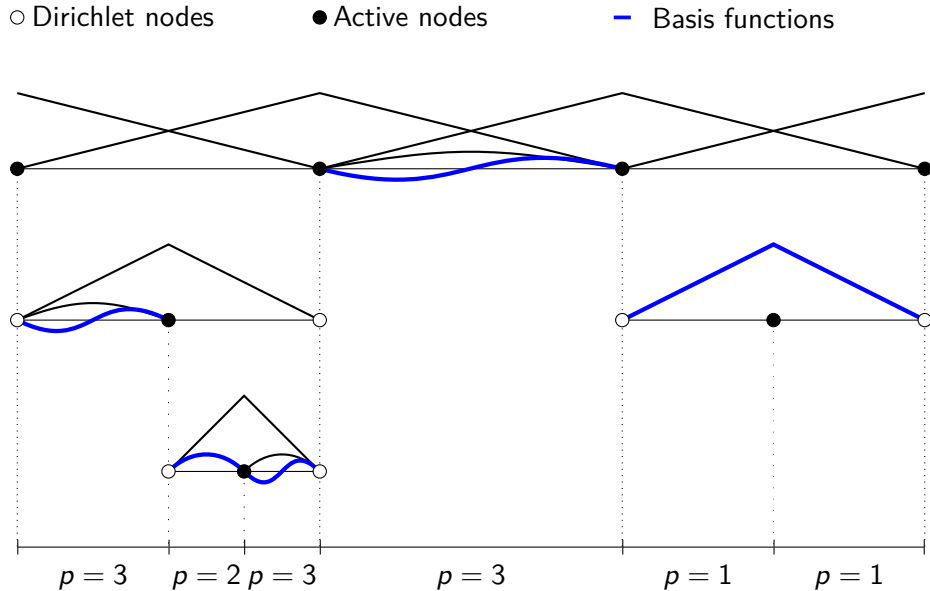


Figure: Main ingredients

Multi-Level Mesh Data Structure 1D



Multi-Level Mesh Data Structure 2D

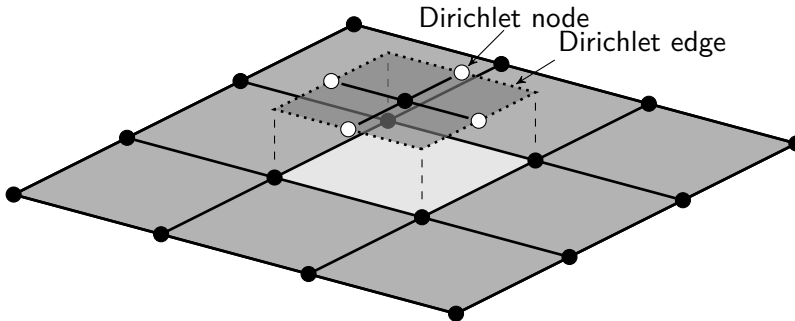


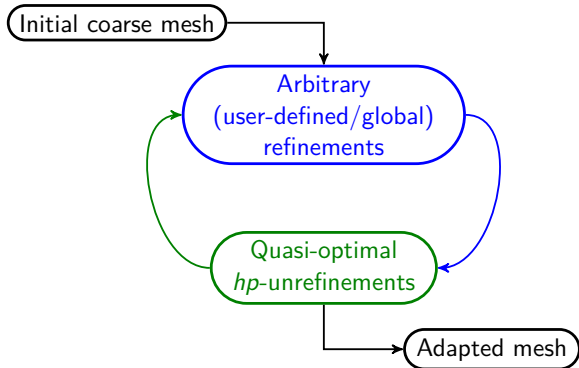
Figure: Multi-level 2D mesh without constraints on hanging nodes using Dirichlet nodes. The bubble basis functions are at the lowest level of each family



N. Zander, T. Bog, S. Kollmannsberger, D. Schillinger, and E. Rank

Multi-level *hp*-adaptivity: high-order mesh adaptivity without the difficulties of constraining hanging nodes
Computational Mechanics, 55(3):499–517, Mar 2015

A Painless Automatic Adaptive Strategy



V. Darrigrand, D. Pardo, T. Chaumont-Frelet, I. Gómez-Revuelto, L. E. García-Castillo

A painless automatic *hp*-adaptive strategy for elliptic problems

Finite Elements in Analysis and Design, 2020.



F. V. Caro, V. Darrigrand, J. Alvarez-Aramberri, E. Alberdi, D. Pardo

A painless multi-level automatic goal-oriented *hp*-adaptive coarsening strategy for elliptic and non-elliptic problems

Computer Methods in Applied Mechanics and Engineering, 2022.

Adaptive Mesh Refinement Algorithm

Algorithm 1: Adaptive process

Input: A given initial mesh

Output: A final hp -adapted mesh

while error above tolerance **do**

 Perform a global and uniform (h or p) refinement;

 Execute a (quasi)-optimal hp -coarsening step (Algorithm 2) to the mesh;

 Update error;

end

hp-Unrefinement Policy

Algorithm 2: *hp*-unrefinement policy

Input: A given mesh

Output: An *hp*-unrefined mesh

do

 Compute the solution on the current mesh;

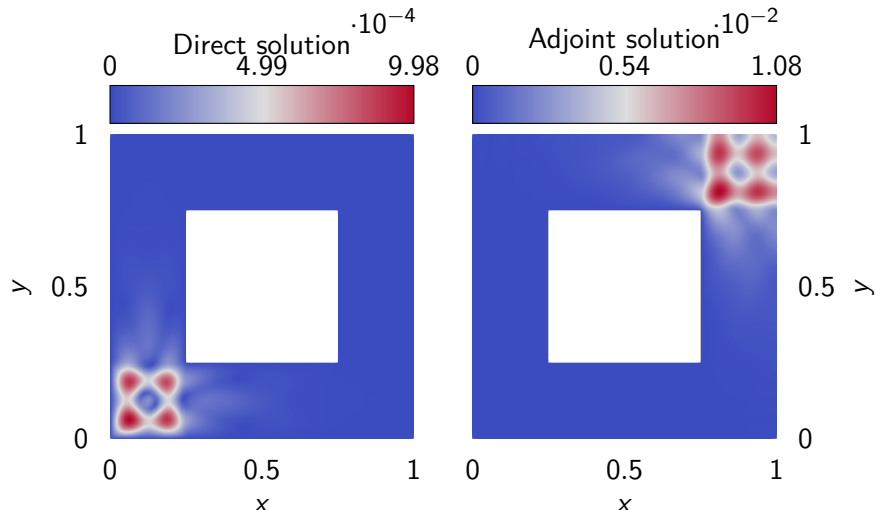
 Compute the element-wise error indicators;

 Unrefine the mesh by eliminating the *removable* basis functions with low error
 indicators;

 When no contributions are below a given tolerance, exit;

end;

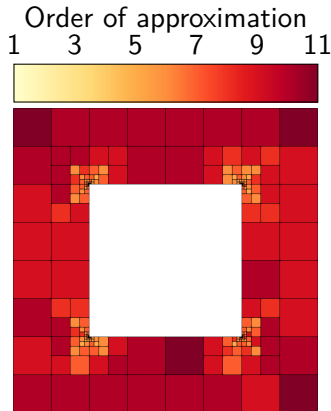
Illustrating the Goal-Oriented hp -Adaptive Strategy



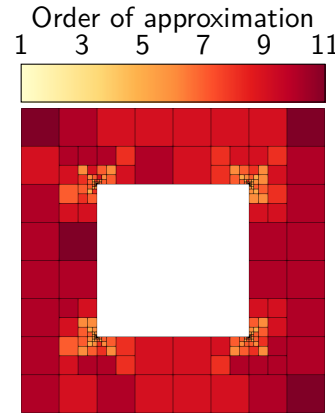
(a) Solution to the direct problem.

(b) Solution to the adjoint problem.

Illustrating the Goal-Oriented *hp*-Adaptive Strategy

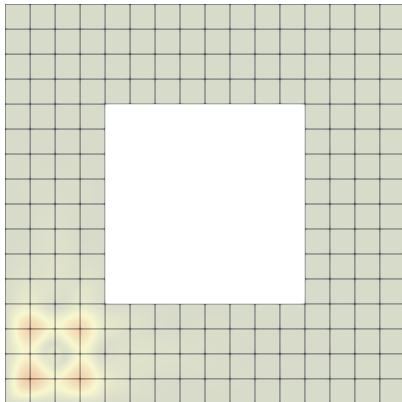


(a) Final *hp*-adapted mesh with polynomial orders in the x-direction.

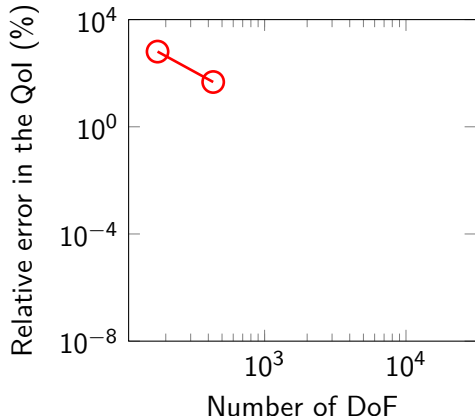


(b) Final *hp*-adapted mesh with polynomial orders in the y-direction.

Illustrating the Goal-Oriented *hp*-Adaptive Strategy



(a) Adaptive iteration 1 of 21



(b) Evolution of the relative error

Figure: Adaptive process for a Helmholtz problem

Illustrating the Goal-Oriented *hp*-Adaptive Strategy

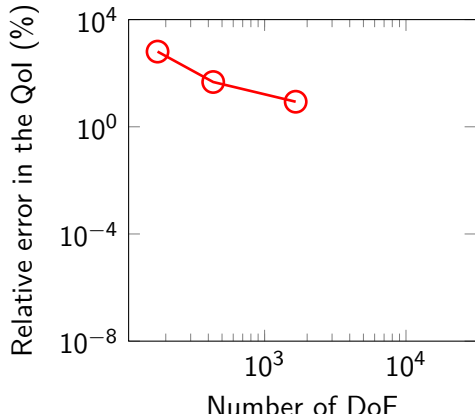
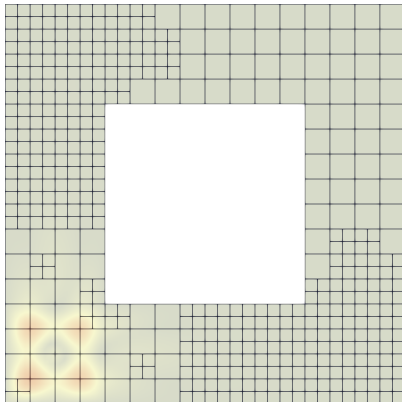
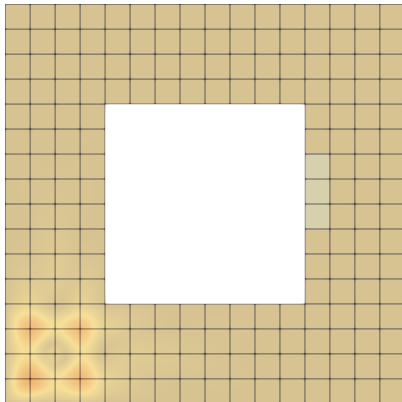
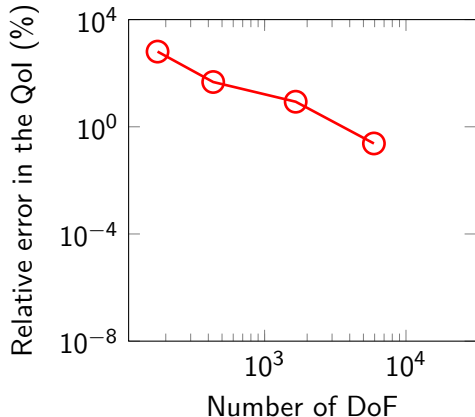


Figure: Adaptive process for a Helmholtz problem

Illustrating the Goal-Oriented hp -Adaptive Strategy



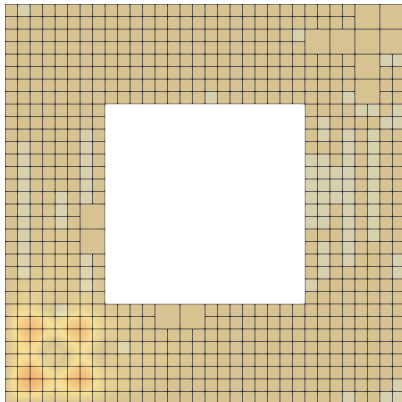
(a) Adaptive iteration 3 of 21



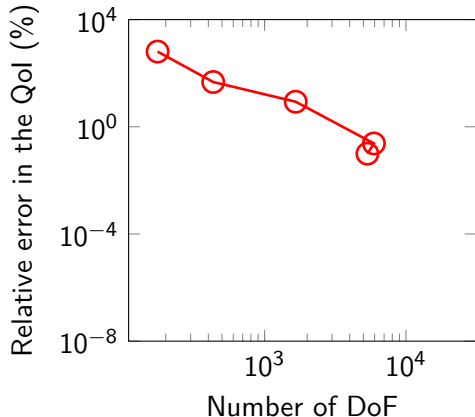
(b) Evolution of the relative error

Figure: Adaptive process for a Helmholtz problem

Illustrating the Goal-Oriented hp -Adaptive Strategy



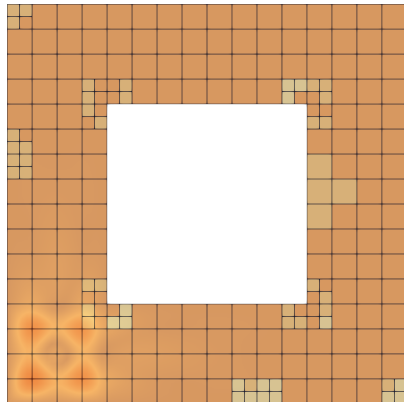
(a) Adaptive iteration 4 of 21



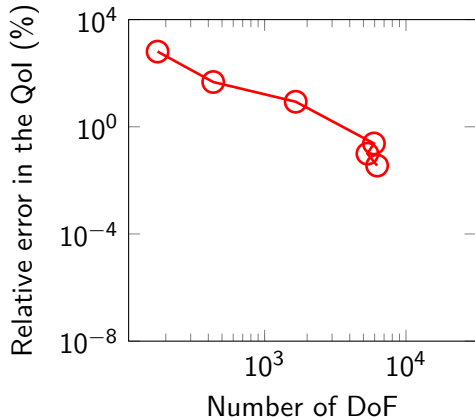
(b) Evolution of the relative error

Figure: Adaptive process for a Helmholtz problem

Illustrating the Goal-Oriented hp -Adaptive Strategy



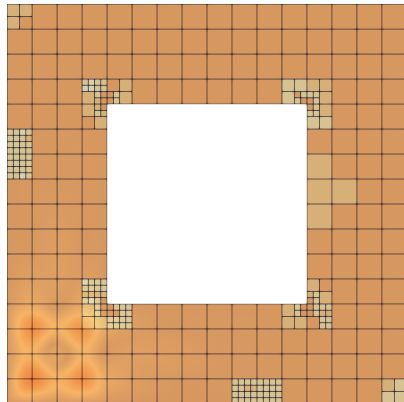
(a) Adaptive iteration 5 of 21



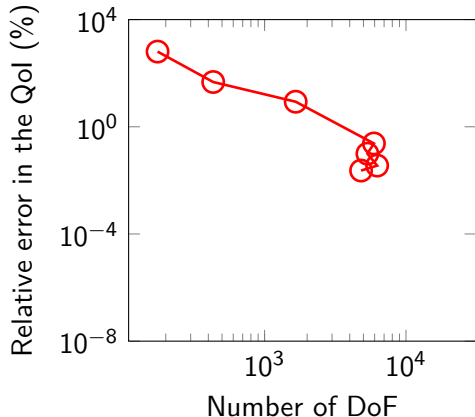
(b) Evolution of the relative error

Figure: Adaptive process for a Helmholtz problem

Illustrating the Goal-Oriented *hp*-Adaptive Strategy



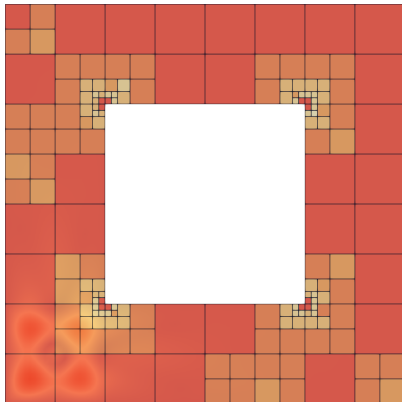
(a) Adaptive iteration 6 of 21



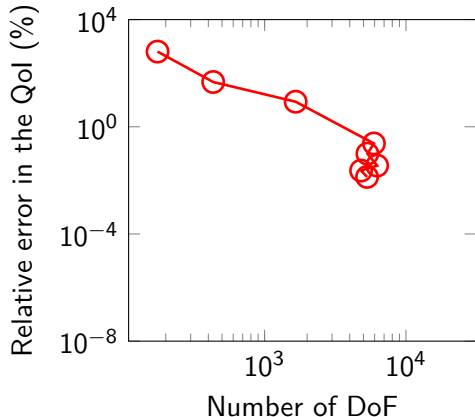
(b) Evolution of the relative error

Figure: Adaptive process for a Helmholtz problem

Illustrating the Goal-Oriented *hp*-Adaptive Strategy



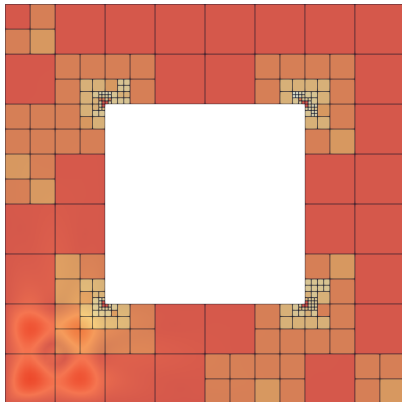
(a) Adaptive iteration 7 of 21



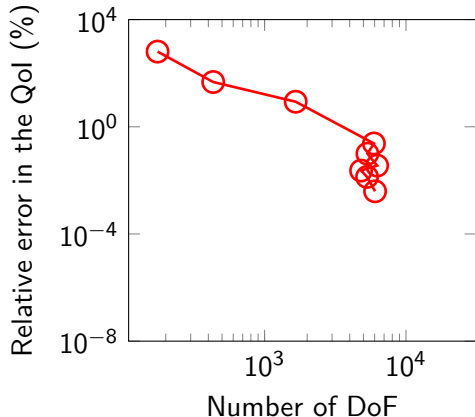
(b) Evolution of the relative error

Figure: Adaptive process for a Helmholtz problem

Illustrating the Goal-Oriented *hp*-Adaptive Strategy



(a) Adaptive iteration 8 of 21



(b) Evolution of the relative error

Figure: Adaptive process for a Helmholtz problem

Illustrating the Goal-Oriented *hp*-Adaptive Strategy

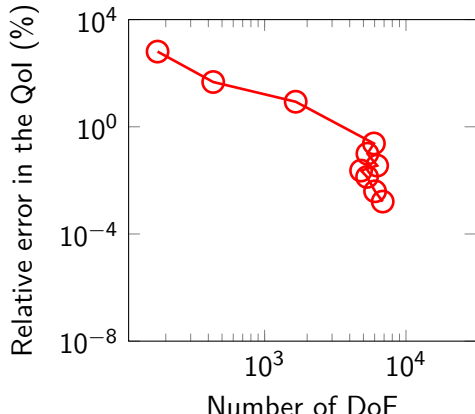
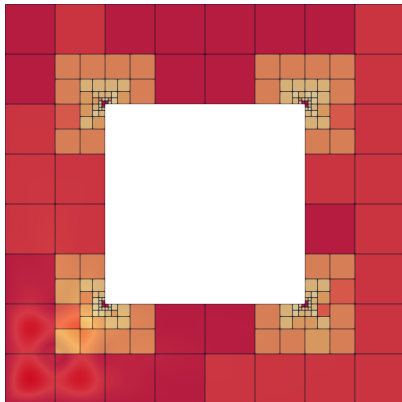
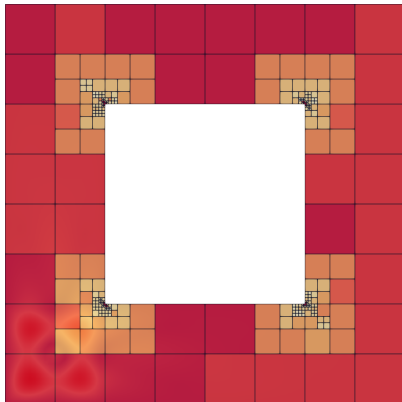
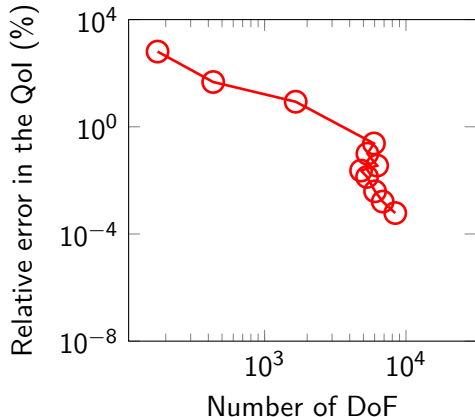


Figure: Adaptive process for a Helmholtz problem

Illustrating the Goal-Oriented *hp*-Adaptive Strategy



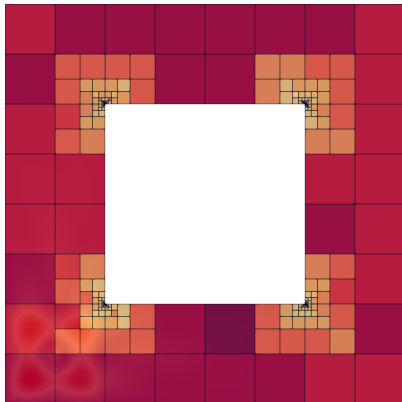
(a) Adaptive iteration 10 of 21



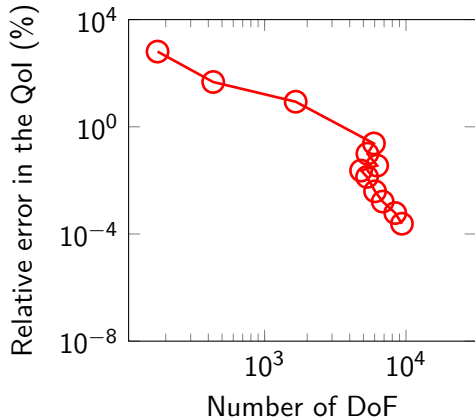
(b) Evolution of the relative error

Figure: Adaptive process for a Helmholtz problem

Illustrating the Goal-Oriented *hp*-Adaptive Strategy



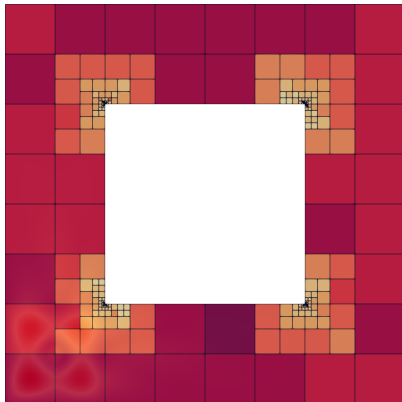
(a) Adaptive iteration 11 of 21



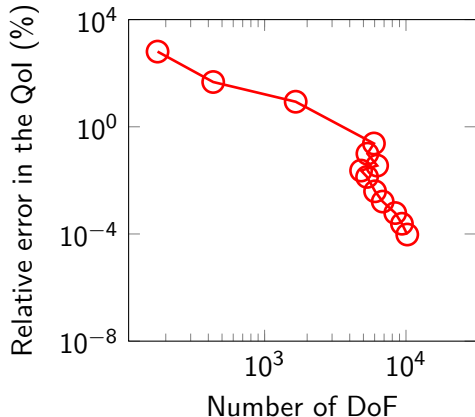
(b) Evolution of the relative error

Figure: Adaptive process for a Helmholtz problem

Illustrating the Goal-Oriented *hp*-Adaptive Strategy



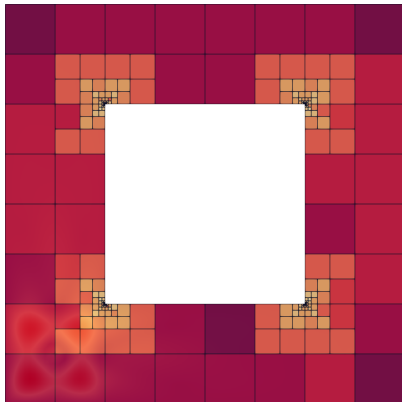
(a) Adaptive iteration 12 of 21



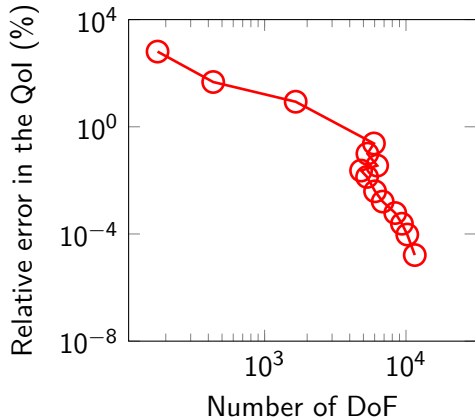
(b) Evolution of the relative error

Figure: Adaptive process for a Helmholtz problem

Illustrating the Goal-Oriented *hp*-Adaptive Strategy



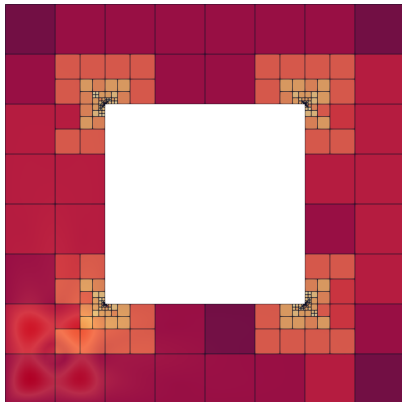
(a) Adaptive iteration 13 of 21



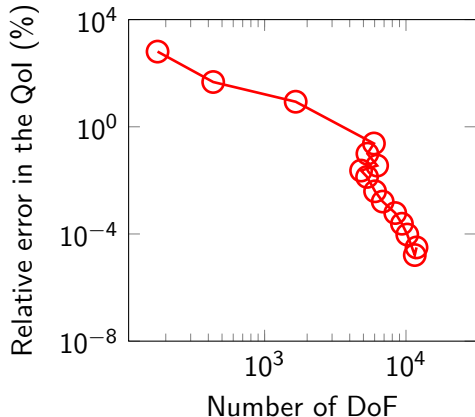
(b) Evolution of the relative error

Figure: Adaptive process for a Helmholtz problem

Illustrating the Goal-Oriented *hp*-Adaptive Strategy



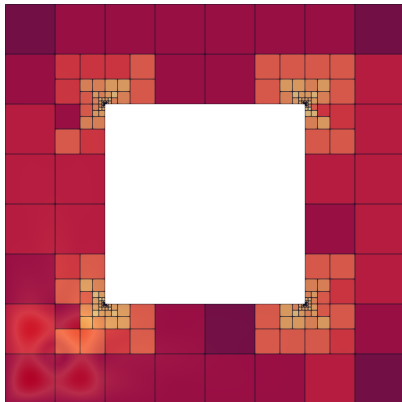
(a) Adaptive iteration 14 of 21



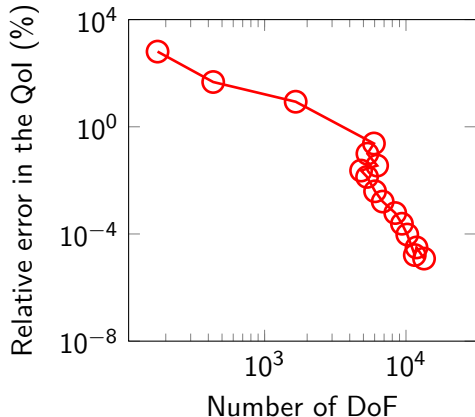
(b) Evolution of the relative error

Figure: Adaptive process for a Helmholtz problem

Illustrating the Goal-Oriented hp -Adaptive Strategy



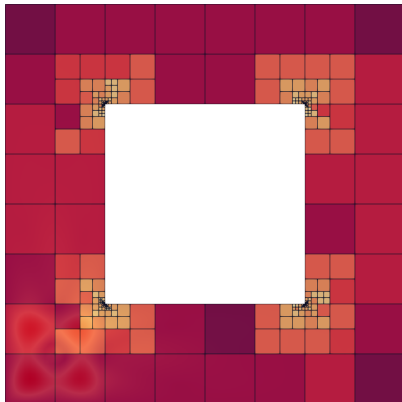
(a) Adaptive iteration 15 of 21



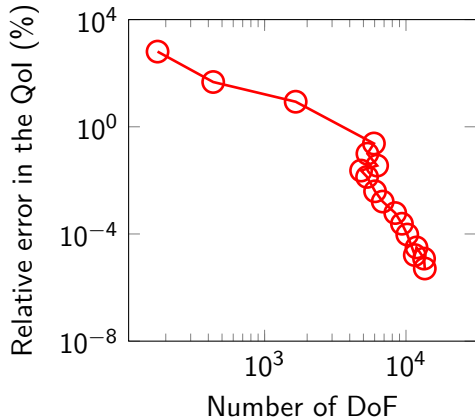
(b) Evolution of the relative error

Figure: Adaptive process for a Helmholtz problem

Illustrating the Goal-Oriented hp -Adaptive Strategy



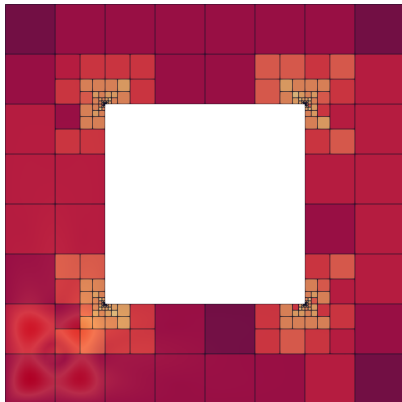
(a) Adaptive iteration 16 of 21



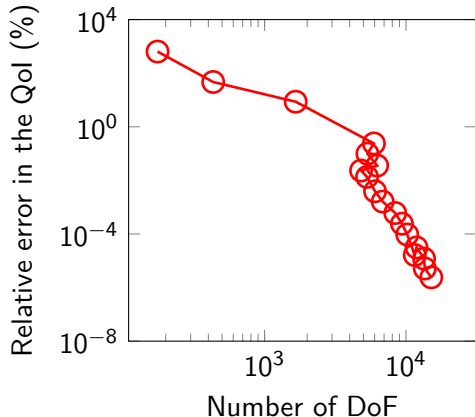
(b) Evolution of the relative error

Figure: Adaptive process for a Helmholtz problem

Illustrating the Goal-Oriented *hp*-Adaptive Strategy



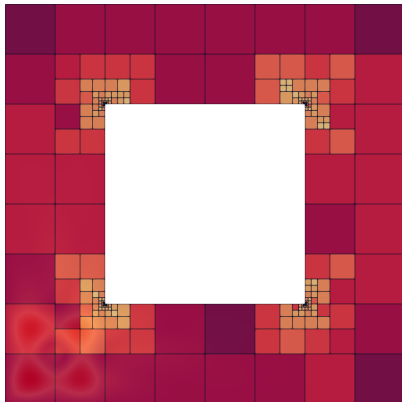
(a) Adaptive iteration 17 of 21



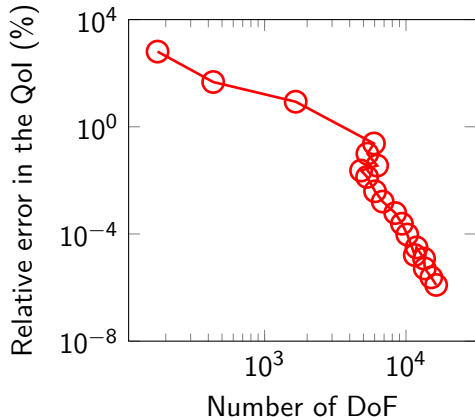
(b) Evolution of the relative error

Figure: Adaptive process for a Helmholtz problem

Illustrating the Goal-Oriented *hp*-Adaptive Strategy



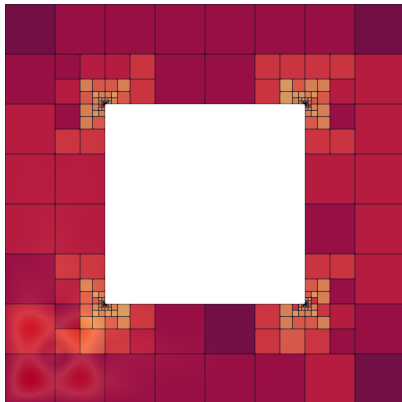
(a) Adaptive iteration 18 of 21



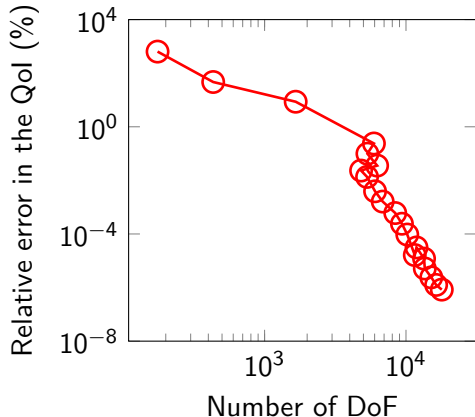
(b) Evolution of the relative error

Figure: Adaptive process for a Helmholtz problem

Illustrating the Goal-Oriented *hp*-Adaptive Strategy



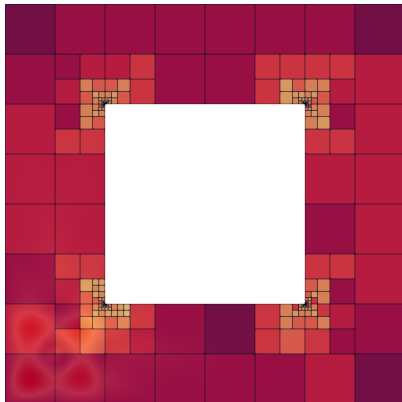
(a) Adaptive iteration 19 of 21



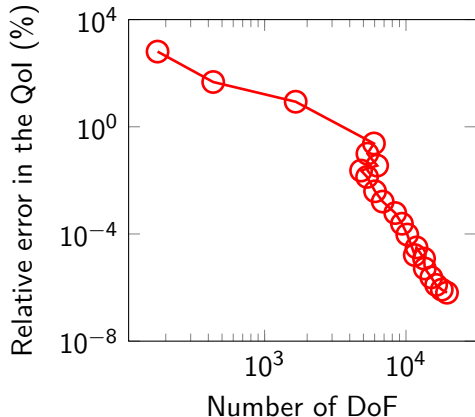
(b) Evolution of the relative error

Figure: Adaptive process for a Helmholtz problem

Illustrating the Goal-Oriented hp -Adaptive Strategy



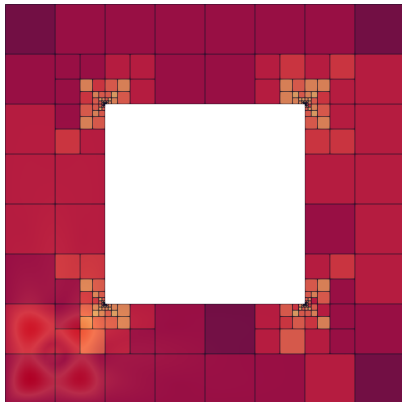
(a) Adaptive iteration 20 of 21



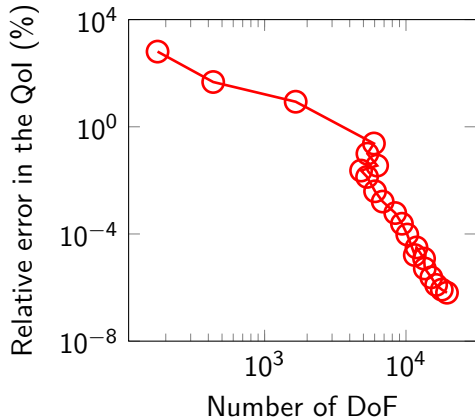
(b) Evolution of the relative error

Figure: Adaptive process for a Helmholtz problem

Illustrating the Goal-Oriented hp -Adaptive Strategy

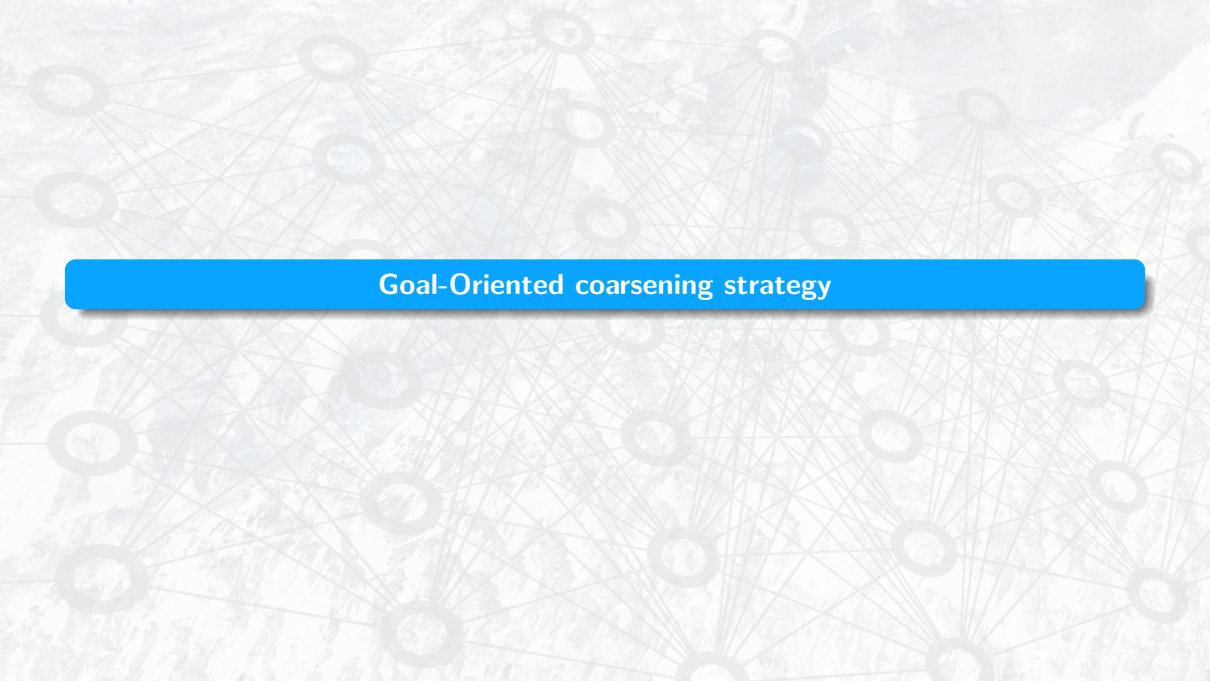


(a) Adaptive iteration 21 of 21



(b) Evolution of the relative error

Figure: Adaptive process for a Helmholtz problem



Goal-Oriented coarsening strategy

The Abstract Variational Formulation

Find $u_{\mathcal{F}} \in \mathbb{H}_{\mathcal{F}}$ such that

$$b(u_{\mathcal{F}}, \phi_{\mathcal{F}}) = f(\phi_{\mathcal{F}}), \quad \forall \phi_{\mathcal{F}} \in \mathbb{H}_{\mathcal{F}}, \quad (1)$$

where:

- $f(\cdot)$ is a linear form,
- b represents a bilinear form defined on $\mathbb{H} \times \mathbb{H}$,
- $\mathbb{H}_{\mathcal{F}} := \text{span}\{\phi_1, \dots, \phi_{n_{\mathcal{F}}}\}$ denotes the finite element space,
- \mathcal{T} represents the discretization of \mathbb{H} into finite elements, where $\mathbb{H}_{\mathcal{F}} \subset \mathbb{H}$,
- $\mathcal{F} = \{\phi_i\}_{i=1}^{n_{\mathcal{F}}}$ is the set of basis functions defining $\mathbb{H}_{\mathcal{F}}$,
- $n_{\mathcal{F}}$ is the dimension of $\mathbb{H}_{\mathcal{F}}$, i.e., $n_{\mathcal{F}} = \dim(\mathbb{H}_{\mathcal{F}})$,
- $u_{\mathcal{F}}$ is the Galerkin approximation of u within $\mathbb{H}_{\mathcal{F}}$.

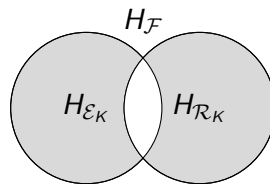
Basis Function Decomposition

Decomposition into Essential and Removable Basis Functions

For any element K , consider the following sets and spaces:

- \mathcal{R}_K : the set of *removable* basis functions associated to K and $|\mathcal{R}_K|$ its cardinality.
- $\mathbb{H}_{\mathcal{R}_K}$: the space generated by \mathcal{R}_K .
- $\mathcal{E}_K := \mathcal{F} \setminus \mathcal{R}_K$: the set of *essential* basis functions.
- $\mathbb{H}_{\mathcal{E}_K}$: the space associated with \mathcal{E}_K .

These satisfy the following properties:



Projection Operator

Definition of the Projection Operator

For a given subset of basis functions $\mathcal{S} \subset \mathcal{F}$ that generates the space $\mathbb{H}_{\mathcal{S}} \subset \mathbb{H}_{\mathcal{F}}$, we define our *projection operator* $\Pi_{\mathcal{F}}^{\mathcal{S}}: \mathbb{H}_{\mathcal{F}} \longrightarrow \mathbb{H}_{\mathcal{S}}$ as

$$\Pi_{\mathcal{F}}^{\mathcal{S}} u_{\mathcal{F}} := \sum_{\phi_i \in \mathcal{S}} u_i \phi_i, \quad (2)$$

where we extract the coefficients of $u_{\mathcal{F}}$ corresponding to the basis functions in \mathcal{S} , and we set the others to zero.

Hence, any function $u_{\mathcal{F}} \in \mathbb{H}_{\mathcal{F}}$ can be decomposed as:

$$u_{\mathcal{F}} = \Pi_{\mathcal{F}}^{\mathcal{E}_K} u_{\mathcal{F}} + \Pi_{\mathcal{F}}^{\mathcal{R}_K} u_{\mathcal{F}}. \quad (3)$$

Note: For a single mesh, the solution $u_{\mathcal{E}_K}$ in \mathcal{E}_K associated with Equation (3) is not computed explicitly. Instead, the projection of $u_{\mathcal{F}}$ onto \mathcal{E}_K is used to approximate it.

Error indicators in our Strategy

Let $\|\cdot\|_e$ be the *energy norm* associated with the Hilbert space \mathbb{H} .

For Elliptic Problems: The energy norm is defined from the bilinear form of the problem b , that is,

$$\|\cdot\|_e^2 = b(\cdot, \cdot).$$

For Non-Elliptic Problems: We define an alternative operator a , not necessarily the original bilinear form, such that

$$|b(\phi, \psi)| \leq |a(\phi, \psi)|, \forall \phi, \psi \in \mathbb{H}$$

and the energy norm is

$$\|\cdot\|_e^2 = a(\cdot, \cdot).$$

The choice of these operators might highly influence the results of the adaptive process, an essential ingredient of adaptive strategies.

Energy-norm based Elliptic Problems

For a given element $K \in \mathcal{T}$, our goal is to quantify the energy lost in the solution when removing a subset of basis functions from the set of *removable* basis functions \mathcal{R}_K .

$$\|u_{\mathcal{F}} - u_{\mathcal{E}_K}\|_e^2.$$

Mathematical Derivation: Analogously to Cea's lemma proof, we derive:

$$\|u_{\mathcal{F}} - u_{\mathcal{E}_K}\|_e^2 = b(u_{\mathcal{F}} - u_{\mathcal{E}_K}, u_{\mathcal{F}} - u_{\mathcal{E}_K}) \quad (4)$$

$$= b(u_{\mathcal{F}} - u_{\mathcal{E}_K}, u_{\mathcal{F}} - \Pi_{\mathcal{F}}^{\mathcal{E}_K} u_{\mathcal{F}}) + b(u_{\mathcal{F}} - u_{\mathcal{E}_K}, \Pi_{\mathcal{F}}^{\mathcal{E}_K} u_{\mathcal{F}} - u_{\mathcal{E}_K}) \quad (5)$$

$$\leq \|u_{\mathcal{F}} - u_{\mathcal{E}_K}\|_e \left\| u_{\mathcal{F}} - \Pi_{\mathcal{F}}^{\mathcal{E}_K} u_{\mathcal{F}} \right\|_e, \quad (6)$$

where we use the b -orthogonality of $u_{\mathcal{F}} - u_{\mathcal{E}_K}$ with $\mathbb{H}_{\mathcal{E}_K}$ and the Cauchy-Schwarz inequality. Hence,

$$\|u_{\mathcal{F}} - u_{\mathcal{E}_K}\|_e \leq \left\| u_{\mathcal{F}} - \Pi_{\mathcal{F}}^{\mathcal{E}_K} u_{\mathcal{F}} \right\|_e = \left\| \Pi_{\mathcal{F}}^{\mathcal{R}_K} u_{\mathcal{F}} \right\|_e. \quad (7)$$

Error Indicator: We define the element-wise error indicator as

$$\eta_K := \left\| \Pi_{\mathcal{F}}^{\mathcal{R}_K} u_{\mathcal{F}} \right\|_e^2, \quad \forall K \in \mathcal{T}. \quad (8)$$

Energy-Based Non-Elliptic Problems

Discrete Inf-Sup Condition: We assume that b satisfies the discrete inf-sup condition:

$$\exists \gamma > 0, \quad \inf_{\phi \in \mathbb{H}_{\mathcal{E}_K}} \sup_{\psi \in \mathbb{H}_{\mathcal{E}_K}} \frac{b(\phi, \psi)}{\|\phi\|_e \|\psi\|_e} \geq \gamma. \quad (9)$$

Utilizing b -Orthogonality: We use the b -orthogonality of $u_{\mathcal{F}} - u_{\mathcal{E}_K}$ with respect to $\mathbb{H}_{\mathcal{E}_K}$.

$$\gamma \left\| \Pi_{\mathcal{F}}^{\mathcal{E}_K} u_{\mathcal{F}} - u_{\mathcal{E}_K} \right\|_e \leq \sup_{\psi \in \mathbb{H}_{\mathcal{E}_K}} \frac{b\left(\Pi_{\mathcal{F}}^{\mathcal{E}_K} u_{\mathcal{F}} - u_{\mathcal{E}_K}, \psi\right)}{\|\psi\|_e} \quad (10)$$

$$\leq M_b \left\| u_{\mathcal{F}} - \Pi_{\mathcal{F}}^{\mathcal{E}_K} u_{\mathcal{F}} \right\|_e, \quad (11)$$

where M_b is the continuity constant of b .

Concluding Inequality: Hence, we derive the following bound:

$$\|u_{\mathcal{F}} - u_{\mathcal{E}_K}\|_e^2 \lesssim \left\| u_{\mathcal{F}} - \Pi_{\mathcal{F}}^{\mathcal{E}_K} u_{\mathcal{F}} \right\|_e^2 = \left\| \Pi_{\mathcal{F}}^{\mathcal{R}_K} u_{\mathcal{F}} \right\|_e^2. \quad (12)$$

Extension to Goal-Oriented Adaptivity

The Adjoint Problem

Find $v_{\mathcal{F}} \in \mathbb{H}_{\mathcal{F}}$ such that

$$b(\phi_{\mathcal{F}}, v_{\mathcal{F}}) = I(\phi_{\mathcal{F}}), \quad \forall \phi_{\mathcal{F}} \in \mathbb{H}_{\mathcal{F}}, \quad (13)$$

where:

- the objective is to produce a space $\mathbb{H}_{\mathcal{F}}$ with minimal dimension such that the error in the Quantity of Interest (QoI) is below a user-defined tolerance,
- the QoI of the solution $u_{\mathcal{F}}$ is expressed as $I(u_{\mathcal{F}})$,
- $v_{\mathcal{F}}$ is the Galerkin approximation of v within $\mathbb{H}_{\mathcal{F}}$,
- $v_{\mathcal{E}_K}$ in \mathcal{E}_K is considered for analysis purposes, but not computed in practice.

Quantifying Changes in the Quantity of Interest (QoI)

For a given element $K \in \mathcal{T}$, we control $|I(u_{\mathcal{F}}) - I(u_{\mathcal{E}_K})|$, $\forall K \in \mathcal{T}$.

Using Galerkin Orthogonality: Since $\mathbb{H}_{\mathcal{E}_K} \subset \mathbb{H}_{\mathcal{F}}$, we have

$$b(u_{\mathcal{F}} - u_{\mathcal{E}_K}, \phi) = 0, \quad \forall \phi \in \mathbb{H}_{\mathcal{E}_K}. \quad (14)$$

Decomposing the Change in QoI:

$$I(u_{\mathcal{F}}) - I(u_{\mathcal{E}_K}) = b(u_{\mathcal{F}} - u_{\mathcal{E}_K}, v_{\mathcal{F}} - v_{\mathcal{E}_K}) \quad (15)$$

$$= b(u_{\mathcal{F}} - u_{\mathcal{E}_K}, \Pi_{\mathcal{F}}^{\mathcal{R}_K} v_{\mathcal{F}}) \quad (\text{second term vanishes}) \quad (16)$$

Applying Decomposition and Orthogonality:

$$|I(u_{\mathcal{F}}) - I(u_{\mathcal{E}_K})| \simeq \left| b(\Pi_{\mathcal{F}}^{\mathcal{R}_K} u_{\mathcal{F}}, \Pi_{\mathcal{F}}^{\mathcal{R}_K} v_{\mathcal{F}}) \right| \leq \left| a(\Pi_{\mathcal{F}}^{\mathcal{R}_K} u_{\mathcal{F}}, \Pi_{\mathcal{F}}^{\mathcal{R}_K} v_{\mathcal{F}}) \right|. \quad (17)$$

Defining Element-wise Indicators:

$$\eta_K := \left| a(\Pi_{\mathcal{F}}^{\mathcal{R}_K} u_{\mathcal{F}}, \Pi_{\mathcal{F}}^{\mathcal{R}_K} v_{\mathcal{F}}) \right|, \quad \forall K \in \mathcal{T}. \quad (18)$$

Error Indicators Using a Pseudo-Dual Operator

The Adjoint Problem

Find $\tilde{\epsilon}$ such that

$$\hat{b}(\phi_{\mathcal{F}}, \tilde{\epsilon}) = I(\phi_{\mathcal{F}}) - b\left(\phi_{\mathcal{F}}, \Pi_{\mathcal{F}}^{\mathcal{E}_K} v_{\mathcal{F}}\right), \quad \forall \phi \in \mathcal{H}, \quad (19)$$

with the following specifications:

- η_K is defined as the error indicator associated with the element K

$$\eta_K := \left| \hat{b}\left(\Pi_{\mathcal{F}}^{\mathcal{R}_K} u_{\mathcal{F}}, \tilde{\epsilon}\right) \right|, \quad \forall K \in \mathcal{T}, \quad (20)$$

- where, the operator $a(\cdot, \cdot)$ is defined as $a(\cdot, \cdot) = \hat{b}(\cdot, \cdot)$.



V. Darrigrand, D. Pardo, I. Muga

Goal-oriented adaptivity using unconventional error representations for the 1D Helmholtz equation

Computers & Mathematics with Applications, 2015

1D Numerical results for Goal-Oriented h - and p -adaptivity

1D Numerical results for Goal-Oriented h - and p -adaptivity

Relative Error

The relative error in the Quantity of Interest (QoI) is defined as:

$$e_{\text{rel}}^{\text{QoI}} := \frac{|I(u) - I(u_{\mathcal{T}_c})|}{|I(u)|} \times 100, \quad (21)$$

where u is the fine grid solution, and $u_{\mathcal{T}_c}$ is the coarser mesh solution.

Helmholtz Goal-Oriented problem

Find u such that:

$$-u'' - k^2 u = \mathbb{1}_{(0, \frac{2}{5})} \quad \text{in } (0, 1), \quad (22)$$

$$u(0) = 0, \quad (23)$$

$$u'(1) = 0. \quad (24)$$

QoI: $I(u) = 5 \int_{\frac{3}{5}}^{\frac{4}{5}} u \, dx$.

Evolution of the Relative Error: h -adaptivity

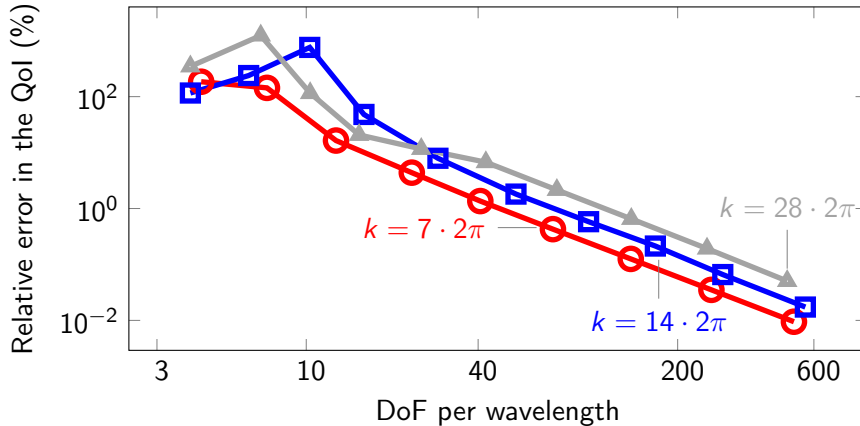


Figure: Evolution of $e_{\text{rel}}^{\text{QoI}}$ using h -adaptivity. Initial mesh size $h = \frac{1}{30}$ and uniform $p = 1$.

Evolution of the Relative Error: p -adaptivity

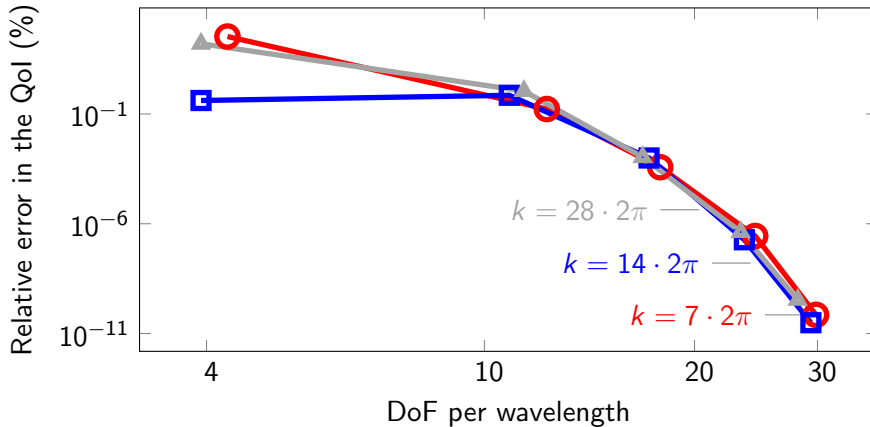


Figure: Evolution of $e_{\text{rel}}^{\text{QoI}}$ using p -adaptivity. Uniform mesh size $h = \frac{1}{30}$.

Solution and Final Adaptive Meshes

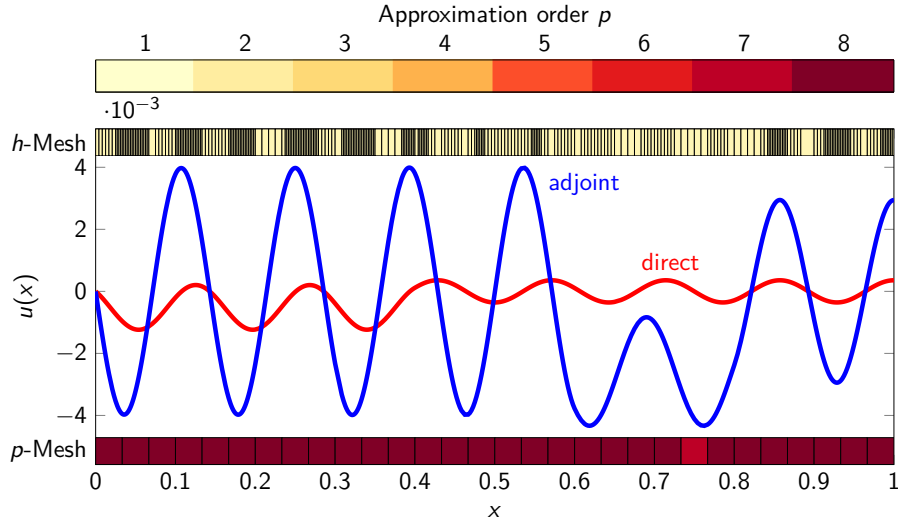


Figure: Solutions with $k = 7 \cdot 2\pi$ problem after the h -adaptive process.

Convection-diffusion Goal-Oriented problem

Find u such that,

$$\begin{aligned} -\varepsilon u'' + \sigma \cdot u' &= \mathbb{1}_{(0,1)} \text{ in } (0, 1), \\ u(0) &= u(1) = 0, \end{aligned} \tag{25}$$

The convection coefficient: $\sigma = 1$.

The diffusive coefficient: $0 < \varepsilon \ll 1$.

QoI: $I(u) = 5 \cdot \int_{\frac{4}{5}}^1 \nabla u \, dx$.

Evolution of the Relative Error: h -adaptivity

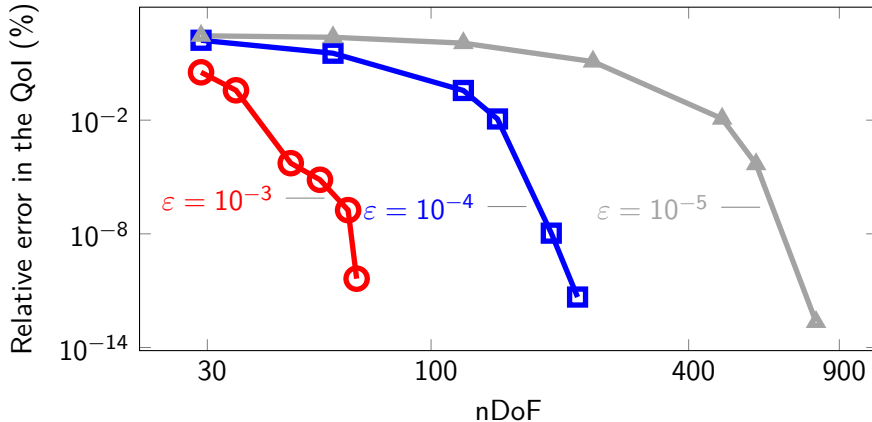


Figure: Evolution of $e_{\text{rel}}^{\text{QoI}}$ using h -adaptivity. Initial mesh size $h = \frac{1}{30}$ and uniform $p = 1$.

Evolution of the Relative Error: p -adaptivity

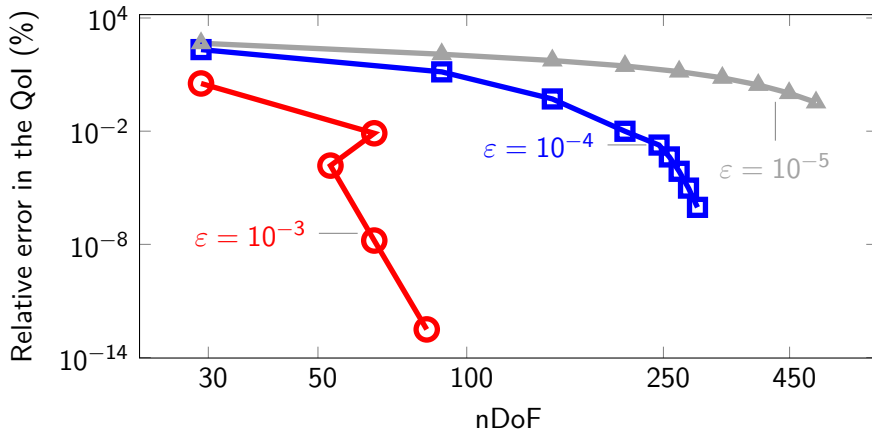


Figure: Evolution of $e_{\text{rel}}^{\text{QoI}}$ using p -adaptivity. Uniform mesh size $h = \frac{1}{30}$.

Solution and Final Adaptive Meshes

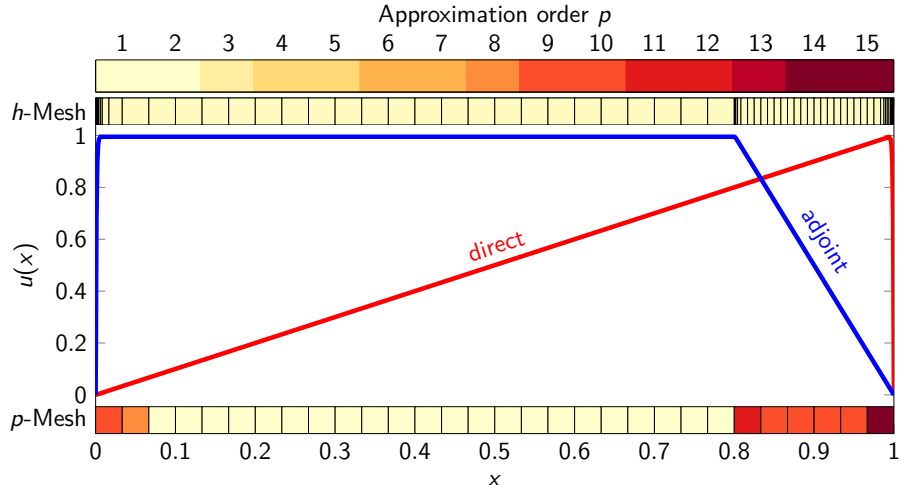


Figure: Solutions with $\varepsilon = 10^{-3}$ problem after the h -adaptive process.

2D Numerical results for hp -adaptivity

2D Numerical results for hp -adaptivity

Lower bound of the relative error

We estimate the following lower bound of the error $e_{\text{rel}}^{\text{energy}}$ as follows:

$$\tilde{e}_{\text{rel}}^{\text{energy}} := \frac{|\|u\|_{\mathbb{H}} - \|u_{\mathcal{T}_c}\|_{\mathbb{H}}|}{\|u\|_{\mathbb{H}}} \cdot 100 \leq e_{\text{rel}}^{\text{energy}} := \frac{\|u - u_{\mathcal{T}_c}\|_{\mathbb{H}}}{\|u\|_{\mathbb{H}}} \cdot 100. \quad (26)$$

Our Quantity of Interest (QoI)

For the GOA problems, we define our QoI as

$$I(\phi) = \frac{1}{|\Omega_I|} \langle \mathbb{1}_{\Omega_I}, \phi \rangle_{L^2(\Omega)}, \quad \forall \phi \in \mathbb{H}, \quad (27)$$

where:

- $|\Omega_I|$ defines the area or volume of Ω_I ,
- $\mathbb{1}_{\Omega_I}$ is a function equal to one if $x \in \Omega_I$, and zero otherwise.

2D Numerical results for hp -adaptivity

Singular Poisson example

Find u satisfying:

$$-\Delta u = \mathbf{1}_{\Omega_f} \quad \text{in } \Omega, \tag{28}$$

$$u = 0 \quad \text{on } \partial\Omega. \tag{29}$$

Domain Definitions:

- $\Omega_f = \left(\frac{1}{4}, \frac{1}{2}\right)^2 \subset \Omega,$
- $\Omega_I = \left(\frac{1}{2}, \frac{3}{4}\right)^2 \subset \Omega,$
- $a(\cdot, \cdot) := \langle \nabla \cdot, \nabla \cdot \rangle_{L^2(\Omega)}.$

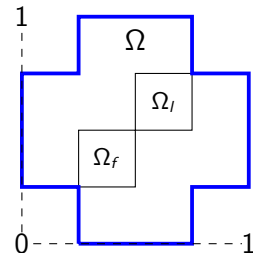
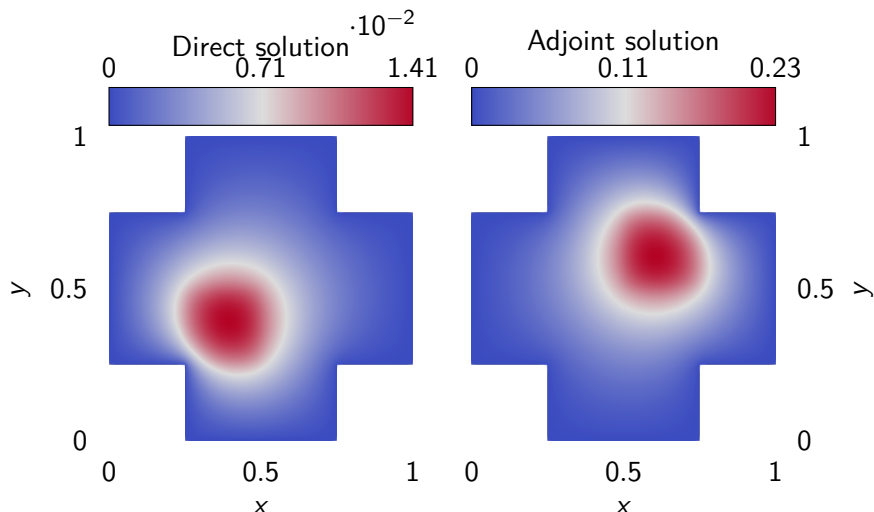


Figure: Domain
 $\Omega = ((0, 1) \times (\frac{1}{4}, \frac{3}{4})) \cup ((\frac{1}{4}, \frac{3}{4}) \times (0, 1)).$

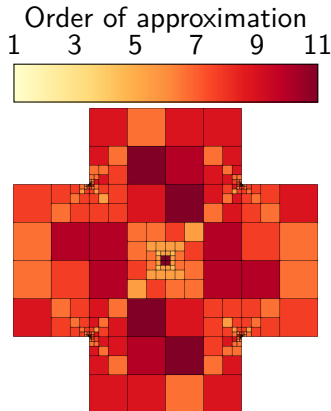
Singular Poisson example



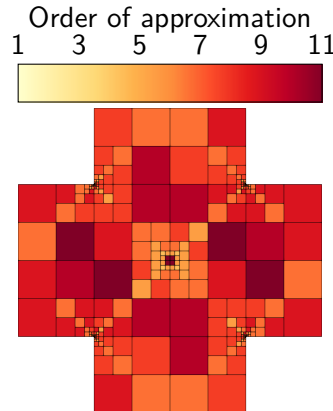
(a) Solution to the direct problem.

(b) Solution to the adjoint problem.

Singular Poisson example



(a) Final *hp*-adapted mesh with polynomial orders in the x-direction.



(b) Final *hp*-adapted mesh with polynomial orders in the y-direction.

Singular Poisson Example

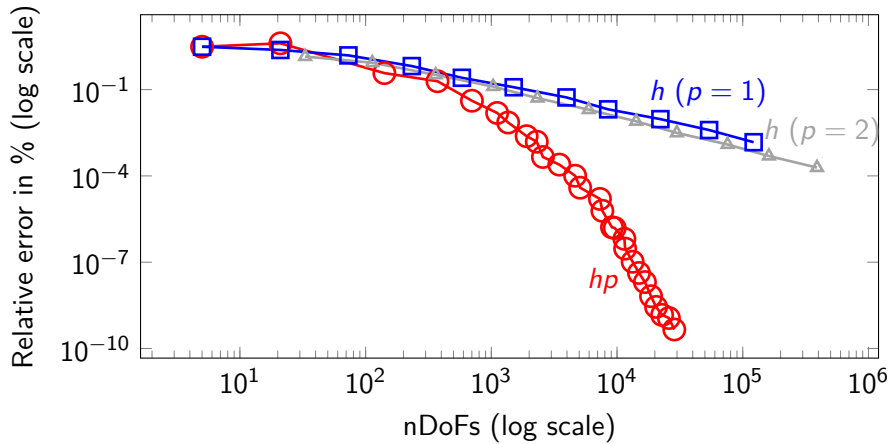


Figure: Evolution of $e_{\text{rel}}^{\text{QoI}}$ in the adaptive process.

2D Numerical results for hp -adaptivity

Wave propagation problem

Find u satisfying:

$$-\Delta u - k^2 u = \mathbb{1}_{\Omega_f} \quad \text{in } \Omega, \quad (30)$$

$$u = 0 \quad \text{on } \Gamma_D, \quad (31)$$

$$\nabla u \cdot \vec{n} = 0 \quad \text{on } \Gamma_N. \quad (32)$$

Domain Definitions:

- $\Omega_f = \left(0, \frac{1}{4}\right)^2 \subset \Omega,$
- $k = (8 \cdot 2\pi, 2\pi),$
- $\Omega_I = \left(\frac{3}{4}, 1\right)^2 \subset \Omega,$
- $a(\cdot, \cdot) :=$

$$\left| \langle \nabla \cdot, \nabla \cdot \rangle_{L^2(\Omega)} \right| + |k^2| \left| \langle \cdot, \cdot \rangle_{L^2(\Omega)} \right|.$$

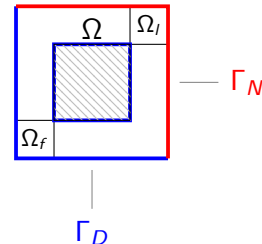
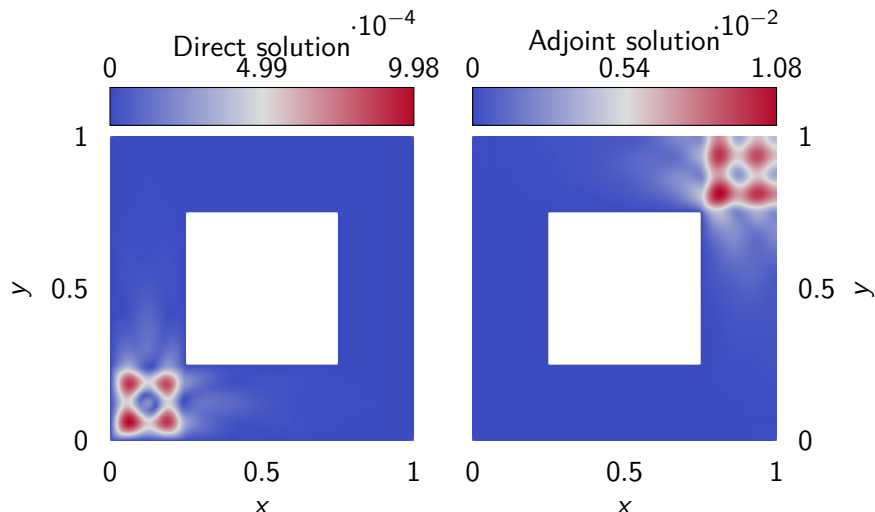


Figure: Domain $\Omega = (0, 1)^2 \setminus \left(\frac{1}{4}, \frac{3}{4}\right)^2 \subset \mathbb{R}^2$.

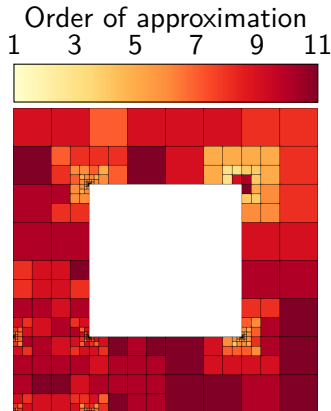
Wave propagation problem



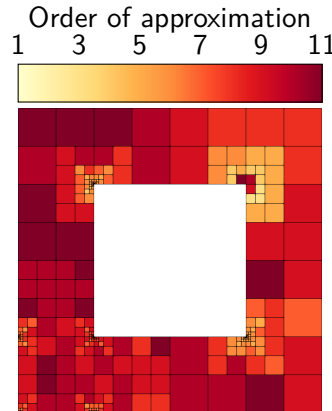
(a) Solution to the direct problem.

(b) Solution to the adjoint problem.

Energy-norm adaptivity



(a) Final hp -adapted mesh with polynomial orders in the x-direction.



(b) Final hp -adapted mesh with polynomial orders in the y-direction.

Energy-norm adaptivity

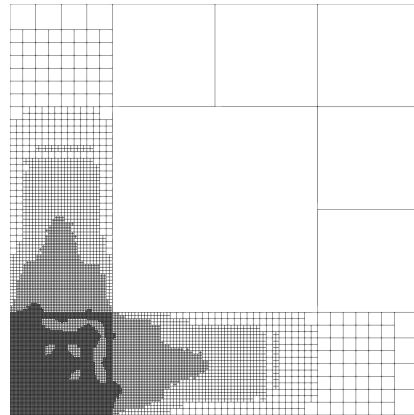
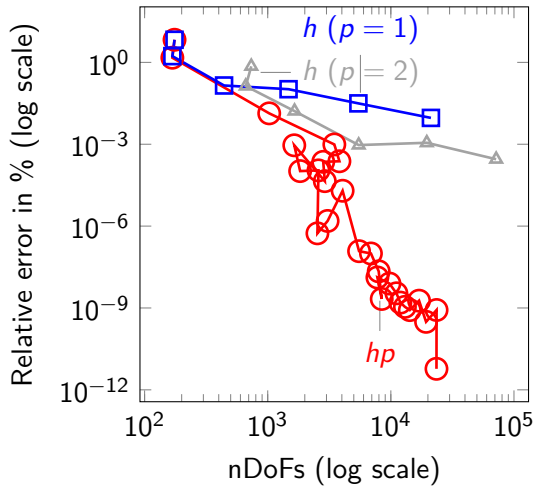
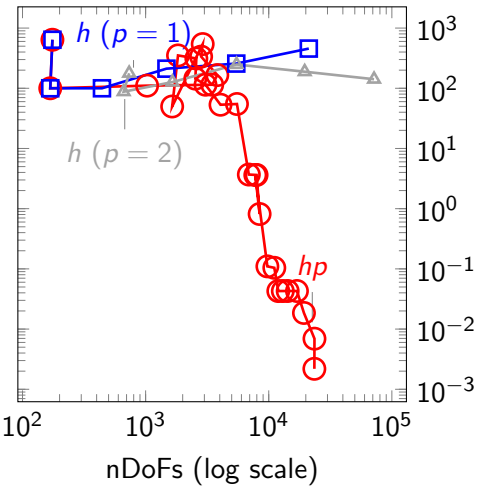


Figure: Final h -adapted mesh for $p = 1$.

Energy-norm adaptivity

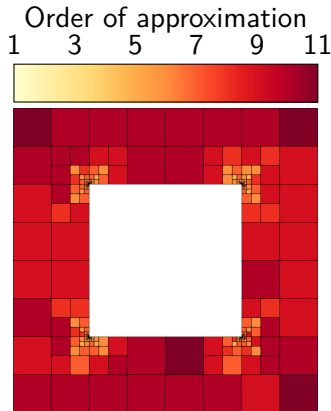


(a) Evolution of $\tilde{e}_{\text{rel}}^{\text{energy}}$ in the process.

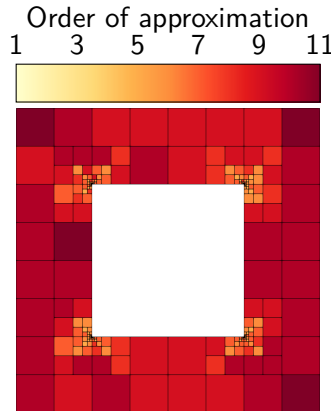


(b) Evolution of $e_{\text{rel}}^{\text{QoI}}$ in the process.

Goal-Oriented adaptivity



(a) Final hp -adapted mesh with polynomial orders in the x-direction.



(b) Final hp -adapted mesh with polynomial orders in the y-direction.

Goal-Oriented adaptivity

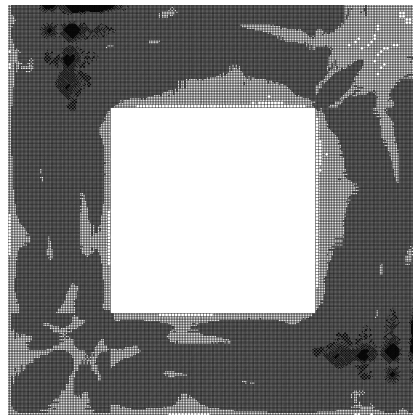
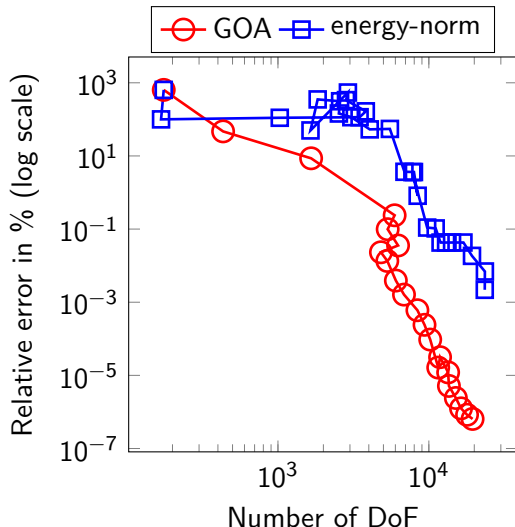
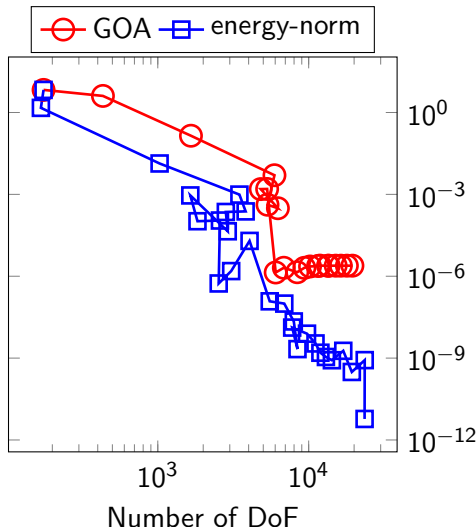


Figure: Final h -adapted mesh for $p = 1$.

Energy-norm and Goal-Oriented hp -adaptive strategy



(a) Evolution of goal-oriented adaptivity.



(b) Evolution of energy-norm adaptivity.

2D Numerical results for hp -adaptivity

Convection-dominated diffusion: example 1

Find u satisfying:

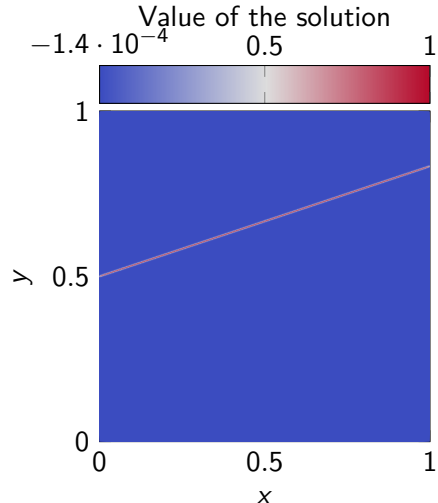
$$-\varepsilon \Delta u + \sigma \cdot \nabla u = f \text{ in } \Omega, \quad (33)$$

$$u = 0 \text{ on } \partial\Omega. \quad (34)$$

Definitions:

- $\Omega = (0, 1)^2 \subset \mathbb{R}^2$,
- $\sigma = (3, 1)^\top$,
- $\varepsilon = 10^{-3}$,
- $u(x, y) = e^{\frac{\varepsilon}{x(x-1)}} \cosh \left(500 \left(\frac{1}{2} + \sigma^{-1}(x, -y) \right) \right)^{-2}$,
- $a(\cdot, \cdot) := (\varepsilon + C) \langle \nabla \cdot, \nabla \cdot \rangle_{L^2(\Omega)}$.

Convection-dominated diffusion: example 1



(a) Solution of the example 1.

Main Achievements

Main Achievements

Peer-Reviewed Publications

-  F. V. Caro, V. Darrigrand, J. Alvarez-Aramberri, and D. Pardo. "A Multi-Adaptive-Goal-Oriented Strategy to Generate Massive Databases of Parametric PDEs," To be submitted to *Computer Methods in Applied Mechanics and Engineering*, December 2023.
-  F. V. Caro, V. Darrigrand, J. Alvarez-Aramberri, E. Alberdi, and D. Pardo. "A Painless Multi-Level Automatic Goal-Oriented hp -Adaptive Coarsening Strategy for Elliptic and Non-Elliptic Problems," *Computer Methods in Applied Mechanics and Engineering*, vol. 401, 115641, 2022. <https://doi.org/10.1016/j.cma.2022.115641>
-  F. V. Caro, V. Darrigrand, J. Alvarez-Aramberri, E. A. Celaya, and D. Pardo. "1D Painless Multi-Level Automatic Goal-Oriented h and p Adaptive Strategies Using a Pseudo-Dual Operator," In *Computational Science – ICCS 2022*, pp. 347–357, 2022.
https://doi.org/10.1007/978-3-031-08754-7_43

Main Achievements

Conference Talks

- [1] F. V. Caro, V. Darrigrand, J. Alvarez-Aramberri, and D. Pardo.
Databases for Deep Learning Inversion Using A Goal-Oriented hp-Adaptive Strategy.
XI International Conference on Adaptive Modeling and Simulation,
Gothenburg, Sweden, June 19-21, 2023.
- [2] F. V. Caro, V. Darrigrand, J. Alvarez-Aramberri, E. Alberdi, and D. Pardo.
*A Painless Automatic hp-Adaptive Coarsening Strategy For Non-SPD problems:
A Goal-Oriented Approach.* 15th World Congress on Computational Mechanics
& 8th Asian Pacific Congress on Computational Mechanics,
Yokohama, Japan, July 31 - August 5, 2022.
- [3] F. V. Caro, V. Darrigrand, J. Alvarez-Aramberri, E. Alberdi, and D. Pardo.
*1D Painless Multi-Level Automatic Goal-Oriented h and p Adaptive Strategies using
a Pseudo-Dual Operator.* 22nd International Conference on Computational Science,
London, United Kingdom, June 21-23, 2022.

Main Achievements

Conference Talks

- [4] F. V. Caro, V. Darrigrand, J. Alvarez-Aramberri, E. Alberdi, and D. Pardo.
Goal-Oriented hp-Adaptive Finite Element Methods: A Painless Multilevel Automatic Coarsening Strategy For Non-SPD Problems. 8th European Congress on Computational Methods in Applied Sciences and Engineering, Oslo, Norway, June 5-9, 2022.
- [5] F. V. Caro, V. Darrigrand, J. Alvarez-Aramberri, E. Alberdi, and D. Pardo.
A Painless Goal-Oriented hp-Adaptive Strategy for Indefinite Problems.
16th U.S. National Congress on Computational Mechanics,
Chicago, U.S.A, July 25-29, 2021.
- [6] F. V. Caro, V. Darrigrand, J. Alvarez-Aramberri, E. Alberdi, and D. Pardo.
Goal-Oriented hp-Adaptive Finite Element Methods: A Painless Multi-level Automatic Coarsening Strategy. 10th International Conference on Adaptive Modeling and Simulation, Gothenburg, Sweden, June 21-23, 2021.

Main Achievements

Research Stays

- FEB. 2023 – MAR. 2023 University of Science and Technology (AGH),
(2 months) Krakow (Poland).
Supervisor: Maciej Paszynski.
- SEP. 2021 – Nov. 2021 CNRS-IRIT-ENSEEIHT (N7),
(2 months) Toulouse (France).
Supervisor: Vincent Darrigrand.
- Nov. 2020 – DEC. 2020 CNRS-IRIT-ENSEEIHT (N7),
(1 month) Toulouse (France).
Supervisor: Vincent Darrigrand.

Main Achievements

Bilbao



Toulouse



Kraków



Conclusions and Future Work

Conclusions

- We employ hierarchical basis functions that effectively address the challenge of *hanging nodes*.
- We have developed **simple-to-implement** h - and p -GOA strategies that use an unconventional symmetric and positive definite bilinear form for possibly non-elliptic goal-oriented problems.
- We have expanded upon a painless automatic hp strategy, initially developed for energy-norm adaptivity, to both non-elliptic and goal-oriented problems.
- We have extended the applicability of a coarsening strategy to encompass parametric PDEs.

Future Work

- Extend algorithms to address multi-physics problems, notably $H(\text{curl})$ and $H(\text{div})$.
- Validate the efficacy of our algorithms in real-world scenarios such as Magnetotellurics, Controlled Sources, and Logging While Drilling.
- Analyze the impact of the nature and distribution of various random samples on DL inversion for optimization.
- Enhance parallelization and factorization techniques to reduce computational resource requirements in future applications.